Inorganic Chemistry

Communication

pubs.acs.org/IC

First Examples of Metal–Organic Frameworks with the Novel 3,3′-(1,2,4,5-Tetrazine-3,6-diyl)dibenzoic Spacer. Luminescence and Adsorption Properties

A. J. Calahorro,[†] Antonio Peñas-Sanjuan,[‡] Manuel Melguizo,[‡] David Fairen-Jimenez,[§] Guillermo Zaragoza,[⊥] Belén Fernández,[∥] Alfonso Salinas-Castillo,[¶] and A. Rodríguez-Diéguez*[,†]

[†]Departamento de Química Inorgánica, Universidad de Granada, Avenida Fuentenueva s/n, 18071 Granada, Spain

[‡]Departamento de Química Inorgánica y Orgánica, Universidad de Jaén, Campus Las Lagunillas, 23071 Jaén, Spain

[§]Department of Chemical & Biological Engineering, Northwestern University, 2145 Sheridan Road, Evanston, Illinois 60208-3120, United States

[⊥]Unidad de Rayos X, RIAIDT Edificio CACTUS, Universidad de Santiago de Compostela, 15782 Santiago de Compostela, Spain

[∥]Instituto de Parasitología y Biomedicina López-Neyra (CSIC), Avenida del Conocimiento s/n, Armilla, Granada

[¶]Departamento de Química Analítica, Universidad de Granada, 18071 Granada, Spain

Supporting Information

ABSTRACT: We report the synthesis of a novel ligand, 3,3′-(1,2,4,5-tetrazine-3,6-diyl)dibenzoic acid (**1**). In this fragment, we have introduced two carboxylate groups with the aim of using this ligand as a linker to construct three-dimensional metal–organic frameworks (MOFs). We have been successful in the formation of zinc (**2**) and lanthanum (**3**) MOFs. The zinc compound is a two-dimensional structure, while the lanthanum material is a three-dimensional MOF with interesting channels. We include the luminescence and adsorption studies of these materials. Moreover, we have evaluated the in vitro toxicity of this novel ligand, concluding that it can be considered negligible.

In the last 15 years, great attention has been paid to metal–organic frameworks (MOFs) as a consequence of their functional properties and potential uses in many applications.[1] Recently, the design and study of zinc- and lanthanum-based MOF has evolved enormously[2] because of their interesting structures and potential applications in areas such as magnetism,[3] luminescence,[4] gas adsorption,[5] sensing, and optical storage.[6] These materials are commonly prepared through a bottom-up approach, using solvothermal methods, connecting transition/lanthanide metal ions with the appropriate bridging ligands. Still, there is great interest in the design of new bridging ligands that will allow the preparation of novel MOFs. Here, we have designed a new symmetrically multidentate bridging ligand, 3,3′-(1,2,4,5-tetrazine-3,6-diyl)dibenzoic acid (**1**; H_2dbtz), which contains two benzoic group donors, bonding to the metals, and a central tetrazine p-acceptor function. Our idea stems from the use of 3,6-disubstituted 1,2,4,5-tetrazine moieties, which have become popular as efficient electronic spacers in dinuclear and polynuclear systems.[7] This is primarily due to the fact that the tetrazine-based low-lying p* orbital conveys strong p-accepting characteristics, leading to excellent electronic communication between the metal termini. In this work, we report the structural, luminescence, and adsorption properties of the first examples of coordination polymers $[Zn(dbtz)(H_2O)]_n$ (**2**) and $\{[La_2(dbtz)_3(H_2O)_2](H_2O)_6\}_n$ (**3**) with the new multidentate ligand H_2dbtz, shown in Scheme S1, demonstrating the potential of this new ligand to construct new MOFs with interesting adsorption properties because of their similarity to other linkers, e.g., NOTT-101 MOF.[8] To the best of our knowledge, these are the first examples of crystal structures of MOFs with ligands that contain the H_2dbtz ligand.

The synthesis (see SI file) of **1** was performed following a variation of the classical Pinner-type scheme in two steps.[9] First, the reaction between 3-cianobenzoic acid and excess hydrazine catalyzed by *N*-acetylcysteine under an inert atmosphere renders the dihydrotetrazine derivative, which was oxidized to give the desired fully aromatic derivative by simple stirring of a methanol suspension of the dihydro derivative in an air atmosphere. Although a similar air oxidation procedure has been reported to aromatize some dihydrotetrazine derivatives,[10] its scope seems to be more general than initially recognized, as proven here.

1 was characterized by ^{1}H and ^{13}C NMR spectrometry [Supporting Information (SI), Figures S1 and S2], electron-impact high-resolution mass spectrometry (HRMS), and X-ray diffraction.[12] Compound **1** crystallizes in the monoclinic space group $P2_1/c$; the asymmetric unit consisting of a medium H_2dbtz ligand that grows by symmetry generated an almost linear alignment between the aromatic rings and terminal carboxylate groups (dihedral angles 3–6°) and one crystallization dimethyl sulfoxide (DMSO) molecule (Figure 1). In the H_2dbtz unit, the bond distances and angles are very similar to those expected in comparison with the tetrazine and benzene rings.[11] In the structure, there is only one type of hydrogen bond (SI, Figure S3), yielding a trinuclear unit formed by one central H_2dbtz unit and two DMSO molecules. In this strong hydrogen bond (O1–H···O3 = 2.565 Å), the oxygen atom pertaining to DMSO and one oxygen atom from the carboxylate group are involved. These

Received: October 20, 2012
Published: January 3, 2013

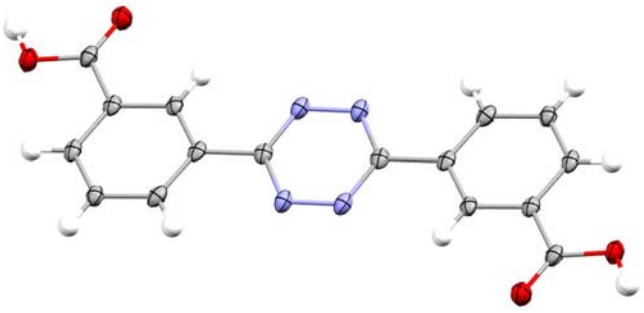

Figure 1. Crystalline structure of **1**. Color code: carbon, gray; nitrogen, blue; oxygen, red; sulfur, yellow; hydrogen, white. The DMSO molecule has been omitted for clarity. Thermal ellipsoids are drawn at the 50% probability level.

trinuclear units are packed through stacking interactions among the tetrazine with benzene rings [3.531(5) Å] and benzene−benzene rings of neighboring units [3.699(5) Å] (SI, Figure S3 and Table S1).

Hydrothermal reactions (see SI file) of the appropriate metal salts (1 mmol) with H_2dbtz (1 mmol) in water (10 mL) at 160 °C for 12 h followed by cooling to room temperature over 3 h yield prismatic pink crystals of **2** (in 57% yield) and **3** (in 75% yield). The crystal structures were determined by single-crystal X-ray crystallography.[12]

Compound **2** consists of double sheets parallel to the *ac* plane. These layers can be described as chains generated by the carboxylate groups, pertaining to the ligand along the *b* directions that are bridged by the $dbtz^{2-}$ spacer. The metal centers have tetrahedral coordination environment ZnO_4 formed by three oxygen atoms, pertaining to three carboxylate groups of three different spacers and one coordinated water molecule.

There are four units of formula $[Zn(dbtz)(H_2O)]$ per cell, and in the crystal structure, each bridging $dbtz^{2-}$ ligand is bound to three metal ions and each metal ion is linked to five other metal ions by three $dbtz^{2-}$ ligands, thus generating stacked double sheets parallel to the [101] direction. The ligand coordinates to the metal center in monodentate and bidentate coordination modes with each carboxylate group, respectively. The coordinated water molecule generates hydrogen bonds with monodentate mode, and infinite two-dimensional networks of the formula $[Zn(dbtz)(H_2O)]_n$ are thus formed; the values of these hydrogen bonds are 2.744(6) and 2.676(6) Å. The association of two such layers by the bidentate mode through one of the carboxylate group bridges gives rise to double layers $[Zn(dbtz)(H_2O)]_n$. These double layers are separated by stacking interactions [3.719(4) Å] (SI, Figure S4 and Table S2). Figure 2 shows a perspective view of the double sheet. The SI, Table S3, gives the main bond lengths and angles.

The crystal structure of **3** consists of a three-dimensional MOF with channels occupied by disordered solvent water molecules

Figure 2. Representation, down [101], of the two-dimensional $[Zn(dbtz)(H_2O)]_n$ layer present in compound **2**.

that propagate along the *a* crystallographic axis. Each La^{III} ion exhibits a LaO_8 coordination environment, which is made of seven oxygen atoms belonging to carboxylate groups of two deprotonated $dbtz^{2-}$ bridging ligands and one coordination water molecule. The $La-O_{water}$ bond distance is 2.82(3) Å, whereas the $La-O_{carb}$ distances are in the range of 2.394(19)−2.564(12) Å. In the structure, lanthanum ions are connected by carboxylate groups pertaining to $dbtz^{2-}$ ligands, generating double chains along the *a*-axis direction. Some oxygen atoms from the carboxylate groups unite two or three lanthanum centers. The dihedral angles between the mean planes of the benzene and tetrazine rings are in the range 7.28−22.67°. These double chains are bridged with six other double chains by $dbtz^{2-}$ ligands.

Each lanthanum ion is linked to 17 other metal ions by 7 $dbtz^{2-}$ ligands, generating a three-dimensional structure (Figure 3). Considering the $dbtz^{2-}$ ligands as spacers and the lanthanum

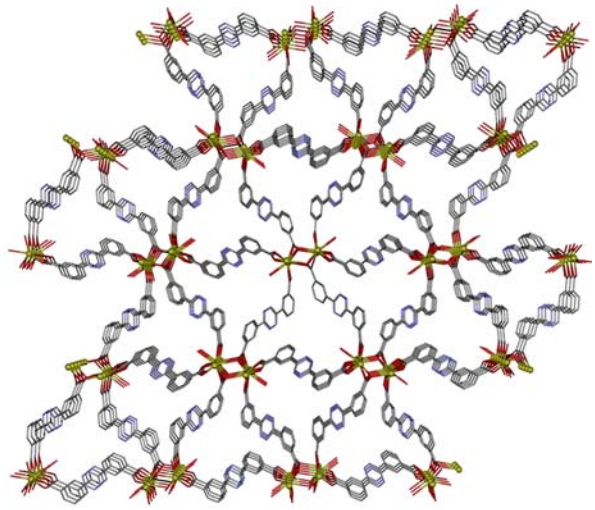

Figure 3. Perspective view along the *a* direction of **3** with the channels in which are located the water molecules. Crystallization water molecules and hydrogen atoms have been omited for clarity.

atoms as nodes, the resulting network generates channels along the *a*-axis direction (SI, Figure S5). These channels have a diameter of 5.02 Å. The shortest and longest La···La distances through $dbtz^{2-}$ spacers are 4.308 and 18.653 Å, respectively.

Thanks to its extended aromaticity and to the presence of polyheterosubstituted hexaatomic rings, H_2dbtz is a good candidate for enhanced emissive properties, tunable, in principle, by coordination to different metals or environments. The emission spectra of compounds **1**−**3** in the solid state at room temperature are shown in (SI, Figure S8). The emission spectra of **1** and **2** at room temperature in the solid state exhibit broad intense emission bands centered at about 454 and 461 nm, respectively, upon excitation at 310 nm. For **3**, using 310 nm incident radiation, intense emission bands at 453 and 470 nm and a stronger one at 498 nm were observed. The emissions in complexes **2** and **3** are assigned to intraligand p−p* transitions, although a considerable red shift is observed with respect to the ligand emission band. Moreover, the emission is more intense than that of the free ligand, which may be explained in terms of the rigidity. The rigidity of the coordinated ligand reduces the loss of energy, thereby increasing the emission efficiency.[13]

We first studied the porous properties of **3** by means of their pore-size distribution (PSD) in a Monte Carlo calculation.[14]

dx.doi.org/10.1021/ic302318j | *Inorg. Chem.* 2013, 52, 546−548

PSD analysis shows that it presents narrow cavities localized at 4 Å (SI, Figure S6). We extended our study by running molecular simulations to predict the adsorption uptake of N_2 and H_2 on **3** at 77 K. Because of the presence of a very narrow porosity, N_2 molecules cannot adsorb in the porosity. On the other hand, the adsorption isotherm of H_2 (SI, Figure S9) predicts an excess capacity at 77 K and 100 bar of 9.97 mg·g^{-1} (12.9 mg·cm^{-3}, using a crystal density of 1.29 g·cm^{-3}). We[15] and others[16] have reported recently high H_2-selective behavior on MOFs for stream purification applications. We studied experimentally the porous structure of **3** after solvent removal, during the adsorption of H_2 at 77 K and up to 100 bar. However, the experimental adsorption isotherm revealed that the porous structure collapsed during activation using conventional methods (heating at 393 K and high vacuum and 10^{-4} bar).

We evaluated the in vitro cytotoxicity of cells exposed to compound **1** at different concentrations and a wide range of incubation times (SI, Figure S7). The results obtained show that for long incubation times and at the highest concentrations analyzed apparent mild signs of toxicity appeared that can be considered negligible with cell viability greater than 80−90%.

These results show that new and interesting materials or MOFs with biomedical applications can be assembled from metal ions and the new H_2dbtz ligand. Work along this line using other paramagnetic/lanthanide metals and X-ray measurements with pressure are in progress in our laboratory. We are also working on the use of a supercritical activation process to allow the removal of solvent molecules from the porosity, keeping the porous texture of the as-prepared material unaffected.

■ ASSOCIATED CONTENT

Ⓢ Supporting Information

X-ray crystallographic data in CIF format, ^{1}H and ^{13}C NMR, crystal structure pictures, computational details, cytotoxicity, preparation of **2** and **3**, luminescence and adsorption graphics, and additional references. This material is available free of charge via the Internet at http://pubs.acs.org. CCDC reference numbers are 902753−902755. The atomic coordinates for these structures have also been deposited with the Cambridge Crystallographic Data Centre. The coordinates can be obtained, upon request, from the Director, Cambridge Crystallographic Data Centre, 12 Union Road, Cambridge CB2 1EZ, U.K.

■ AUTHOR INFORMATION

Corresponding Author

*E-mail: antonio5@ugr.es.

Notes

The authors declare no competing financial interest.

■ ACKNOWLEDGMENTS

This work was supported by the Junta de Andalucía (Predoctoral Grant FQM-4228 to A.J.C.), the University of Granada, and the Department of Energy's Office of Energy Efficiency and Renewable Energy, Fuel Cell Technologies Program under Grant DE-FC36-08GO18137. B.F. thanks to the MEC for the postdoctoral contract "Juan de la Cierva".

■ REFERENCES

(1) (a) Kondo, A.; Noguchi, H.; Kajiro, H.; Carlucci, L.; Mercandelli, P.; Proserpio, D. M.; Tanaka, H.; Kaneko, K.; Kanoh, H. *J. Phys. Chem. B* **2006**, *110*, 25565−25567. (b) Rowsell, J. L. C.; Yaghi, O. M. *J. Am. Chem. Soc.* **2006**, *128*, 1304. (c) Hong, M. *Cryst. Growth Des.* **2007**, *7*, 10. (d) Vertova, A.; Cucchi, I.; Fermo, P.; Porta, F.; Proserpio, D. M.; Rondinini, S. *Electrochim. Acta* **2007**, *52*, 2603−2611. (e) Janiak, C. *Dalton Trans.* **2003**, *14*, 2781. (f) Yang, S.; Sun, J.; Ramirez-Cuesta, A. J.; Callear, S. K.; David, W. I. F.; Anderson, D. P.; Newby, R.; Blake, A. J.; Parker, J. E.; Tang, C. C.; Schröder, M. *Nat. Chem.* **2012**, *4*, 887−894. (g) Long, J. R.; Yaghi, O. M. *Chem. Soc. Rev.* **2009**, *38*, 1201−1507.

(2) (a) Almeida Paz, F. A.; Klinowski, J. *Chem. Commun.* **2003**, 1484−1485. (b) Long, D.-L.; Blake, A. J.; Champness, N. R.; Wilson, C.; Schröder, M. *Angew. Chem., Int. Ed.* **2001**, *40*, 2444−2447. (c) Ma, B.-Q.; Zhang, D.-S.; Gao, S.; Jin, T.-Z.; Yan, C.-H.; Xu, G.-X. *Angew. Chem., Int. Ed.* **2000**, *39*, 3644−3646.

(3) (a) Morrish, A. H. *The Physical Principles of Magnetism*; Wiley: New York, 1965. (b) Chen, Z.; Zhao, B.; Zhang, Y.; Shi, W.; Cheng, P. *Cryst. Growth Des.* **2008**, *8*, 229−233.

(4) (a) Shunmugam, R.; Tew, G. N. *J. Am. Chem. Soc.* **2005**, *127*, 13567−13572. (b) Rosi, N. L.; Kim, J.; Eddaoudi, M.; Chen, B. L.; O'Keeffe, M.; Yaghi, O. M. *J. Am. Chem. Soc.* **2005**, *127*, 1504−1518.

(5) (a) Pan, L.; Adams, K. M.; Hernandez, H. E.; Wang, X.; Zheng, C.; Hattori, Y.; Kaneko, K. *J. Am. Chem. Soc.* **2003**, *125*, 3062−3067. (b) Dawson, R.; Adams, D. J.; Cooper, A. I. *Chem. Sci.* **2011**, *2*, 1173−1177.

(6) (a) Kuriki, K.; Koike, Y.; Okamoto, Y. *Chem. Rev.* **2002**, *102*, 2347−2356. (b) Bünzli, J. C. G.; Piguet, C. *Chem. Soc. Rev.* **2005**, *34*, 1048−1077. (c) Robin, A. Y.; Fromm, K. M. *Coord. Chem. Rev.* **2006**, *250*, 2127−2157.

(7) Kaim, W. *Coord. Chem. Rev.* **2002**, *230*, 127−139.

(8) Lin, X.; Telepeni, I.; Blake, A. J.; Dailly, A.; Brown, C. M.; Simmons, J. M.; Zoppi, M.; Walker, G. S.; Thomas, K. M.; Mays, T. J.; Hubberstey, P.; Champness, N. R.; Schröder, M. *J. Am. Chem. Soc.* **2009**, *1331*, 2159−2171.

(9) Pinner, A.; Liebig, J. *Ann. Chem.* **1897**, *297*, 221−271.

(10) Cutivet, A.; Leroy, E.; Pasquinet, E.; Poullain, D. *Tetrahedron Lett.* **2008**, *49*, 2748−2751.

(11) Kaszynski, P.; Young, V. G. *J. Am. Chem. Soc.* **2000**, *122*, 2087−2090.

(12) Crystal data for **1** ($C_{20}H_{22}N_4O_6S_3$), M = 478.56, triclinic, space group $P\bar{1}$, a = 6.3054(6) Å, b = 8.0715(9) Å, c = 11.4005(13) Å, α = 73.397(7)°, β = 82.195(7)°, γ = 85.851(7)°, V = 550.53(10) Å^3, Z = 1, ρ_{calcd} = 1.443 g·cm^{-3}, μ(Mo Kα) = 0.287 mm^{-1}, R1(F_o) = 0.0598, and wR2(F_o^2) = 0.1468 with a GOF on F^2 = 1.015. Crystal data for **2** ($C_{16}H_{10}N_4O_5Zn$): M = 403.67, monoclinic, space group $P2_1/n$, a = 7.247(4) Å, b = 6.814(4) Å, c = 29.631(17) Å, β = 90.015(9)°, V = 1463.3(15) Å^3, Z = 4, ρ_{calcd} = 1.832 g·cm^{-3}, μ(Mo Kα) = 1.72 mm^{-1}, R1(F_o) = 0.0495, and wR2(F_o^2) = 0.1113 with a GOF on F^2 = 1.02. Crystal data for **3** ($C_{24}H_{12}N_6O_{10}La$): M = 683.31, monoclinic, space group $P2_1/c$, a = 5.1474(10) Å, b = 18.232(4) Å, c = 26.783(5) Å, β = 90.08(3)°, V = 2513.5(9) Å^3, Z = 4, ρ_{calcd} = 1.806 g·cm^{-3}, μ(Mo Kα) = 1.771 mm^{-1}, R1(F_o) = 0.0727, and wR2(F_o^2) = 0.1677 with a GOF on F^2 = 1.034. Data were collected by ω and ψ scans on a Bruker APEXII diffractometer with graphite-monochromated Mo Kα radiation (λ = 0.71073 Å). The structures were solved by direct methods and refined on F^2 by the *SHELX-97* program.

(13) (a) Aldridge, S.; Downs, A. J. *The Group 13 Metals Aluminium, Gallium, Indium and Thallium*; John Wiley & Sons: New York, 2011. (b) Rodríguez-Diéguez, A.; Salinas-Castillo, A.; Sironi, A.; Seco, J. M.; Colacio, E. *CrystEngComm* **2010**, *12*, 1876−1879. (c) Tan, B.; Xie, Z.-L.; Feng, M.-L.; Hu, B.; Wu, Z.-F.; Huang, X.-Y. *Dalton Trans.* **2012**, *41*, 10576−10584.

(14) (a) Gelb, L. D.; Gubbins, K. E. *Langmuir* **1999**, *15*, 305. (b) Düren, T.; Millange, F.; Férey, G.; Walton, K. S.; Snurr, R. Q. *J. Phys. Chem. C* **2007**, *111*, 5350−5357.

(15) Calahorro, A. J.; López-Viseras, M. E.; Salinas-Castillo, A.; Fairen-Jimenez, D.; Colacio, E.; Cano, J.; Rodríguez-Diéguez, A. *CrystEngComm* **2012**, *14*, 6390−6393.

(16) (a) Chen, B.; Ma, S.; Zapata, F.; Fronczek, F. R.; Lobkovsky, E. B.; Zhou, H. C. *Inorg. Chem.* **2007**, *46*, 1233−1236. (b) Xue, M.; Ma, S.; Jin, Z.; Schaffino, R. M.; Zhu, G. S.; Lobkovsky, E. B.; Qiu, S. L.; Chen, B. L. *Inorg. Chem.* **2008**, *47*, 6825−6828.